Supporting Information

N-Doped CoO-anchored Ultrafine Pt Nanoparticles for

Acidic Hydrogen Evolution Reaction

*Xin Wen [a], Dewen Wang [b], Jinchang Fan [a], Tianyi Gao [a], Xinyi Li [a], Yanhua Liu [a], Xiaowen Ruan [c] and Xiaoqiang Cui [a] ***

a. *School of Materials Science and Engineering, Key Laboratory of Automobile Materials of MOE, Jilin Provincial International Cooperation Key Laboratory of High-Efficiency Clean Energy Materials, Jilin University, Changchun 130012, China.*

b. *State Key Laboratory of Electroanalytical Chemistry, Changchun Institute of Applied Chemistry, Chinese Academy of Sciences, Changchun 130022, P. R.China.*

c. *School of Energy and Environment, City University of Hong Kong, Tat Chee Avenue, Kowloon, Hong Kong SAR.*

[*] Corresponding Author: Prof. Xiaoqiang Cui,

E-mail: xqcui@jlu.edu.cn (X. Q. Cui)

Experimental

1. Materials

2-Methylimidazole ($C_4H_6N_2$, 98%) and Sodium tetrachloroplatlnate(II) Hydrate ($Na_2PtCl_4 \cdot xH_2O$) were sourced from Shanghai Aladdin Biochemical Technology Co., Ltd., China. Hexade cylyrimethyl ammonium chloride ($C_{19}H_{42}CIN$, CP) and Cobalt(II) nitrate hexahydrate ($Co(NO_3)_2 \cdot 6H_2O$, AR) were purchased from Sinopharm Chemical Reagent Co., China. Cobalt(II) hydroxide ($Co(OH)_2$, 98%) was acquired from Shanghai Macklin Biochemical Co.,Ltd., (China). The Nafion-ethanol solution was obtained from Adamas-beta Chemical Co., Switzerland. A Commercial Pt/C catalyst (20 wt. %) was sourced from Johnson Mattkey (UK). High-purity Argon (Ar, 99.999%) was purchased from Xin'guang Gas Co., China.

2. Synthesis of the ZIF-67

In the standard experiment protocol, a solution was prepared by dissolving 580 mg of cobalt(II) nitrate hexahydrate ($Co(NO_3)_2 \cdot 6H_2O$) in 20 mL of deionized (DI) water containing 30 mg of hexadecyltrimethylammonium bromide (CTAB). Subsequently, this solution was injected into a separate aqueous solution consisting of 9.08 g of 2-methylimidazole in 140 mL, followed by stirring at room temperature for 60 minutes. The resulting purple precipitate was collected through centrifugation and subsequently washed with ethanol five times.

3. Synthesis of the Pt-N-CoO Catalysts

To prepare the Pt-N-CoO catalyst, an ion exchange process was conducted prior to pyrolysis. In this procedure, 100 mg of ZIF-67 nanocrystals were dispersed in 50 mL of DI water. Subsequently, 0.02 mmol of disodium tetrachloroplatinate hydrate ($Na_2PtCl_4 \cdot xH2O$) was slowly added to the ZIF-67 solution under stirring conditions. After 3 hours, the reaction was halted by centrifuging the suspension. The resulting precipitate was collected, washed twice with DI water, and then thrice with ethanol. The Pt-N-CoO nanosheets were acquired by drying the precipitate at 60 °C overnight in a vacuum oven followed pyrolysis at 300 °C in an argon atmosphere for 4 hours.

4. Synthesis of the Pt-CoO Catalysts

100 mg of $Co(OH)_2$ was dispersed in 50 mL of DI water. Subsequently, 0.04 mmol of disodium tetrachloroplatinate hydrate ($Na_2PtCl_4·xH2O$) were slowly added into the $Co(OH)_2$ solution under stirring conditions. The resulting mixture was then refluxed at 80 °C in an oil bath with magnetic stirring for 4 hours. After the reaction, the suspension was centrifuged to collect the precipitate which was then washed twice with DI water followed by three washes with ethanol. The obtained Pt-CoO nanosheets were dried at 60 °C overnight in a vacuum oven and then pyrolyzed at 300 °C in argon atmosphere for 4 hours.

5. Characterization

Transmission electron microscopy (TEM) and high resolution transmission electron microscopy (HRTEM) images were acquired using a JEM-2100F transmission electron microscope (JEOL, Japan). Scanning electron microscope (SEM) images and corresponding energy-dispersive X-ray (EDX) mapping were obtained with a Hitachi SU8010 scanning microscope operating at an accelerating voltage of 5 kV. X-ray photoelectron spectroscopy (XPS) data was acquired with an ESCALAB-250 instrument (Thermo Fisher Scientific, USA). The measurements were performed with a monochromatic Al-Kα (1486.6 eV) radiation source and a hemisphere detector with an energy resolution of 0.1 eV. Inductively coupled plasma mass spectrometry (ICP-MS) data was collected with an ELAN 9000/DRC system. X-ray diffraction(XRD) patterns were obtained using a Bragg–Brentano diffractometer (D8-tools, Germany). Raman tests were conducted using an inVia (Renishaw Company) instrument with irradiation at 532 nm. The X-ray absorption fine structure spectra (XAFS) of the Pt L3-edge and Co K-edge were collected at 1W1B station in Beijing Synchrotron Radiation Facility (BSRF).

6. Electrochemical measurements and product analysis

All electrochemical tests were conducted using CHI 760E electrochemical workstation (CH Instruments, Inc., Shanghai) in a 0.5 M H_2SO_4 solution. The conventional three-electrode system was utilized for evaluating the electrochemical HER performance. The working electrode consisted of a carbon paper electrode coated

with the catalyst, while a carbon rod served as the counter electrode. All electrochemical potentials in this study were referenced to the reversible hydrogen electrode (RHE) and were calculated by the following equation: E(RHE)=E(Hg/Hg$_2$Cl$_2$)+0.242+0.059 pH. The HER polarization curves were obtained by linear voltammetry (LSV) technique and were corrected using the automatic iR compensation function of the workstation. The electrochemical impedance spectra (EIS) were obtained in the frequency range of 100000-0.01 Hz with an AC amplitude of 5 mV. The loading amounts for as-prepared catalysts was 0.4 mg/cm^2. Mass activity

$= \dfrac{j}{m \times c}$, where j represents the current density (A cm^{-2}) contributed by the Pt active sites at an overpotential of 50 mV, m shows the mass loading of the electrocatalyst (mg), and c indicates the mass content of Pt in catalysts. The relevant content was added in the revised supporting information.
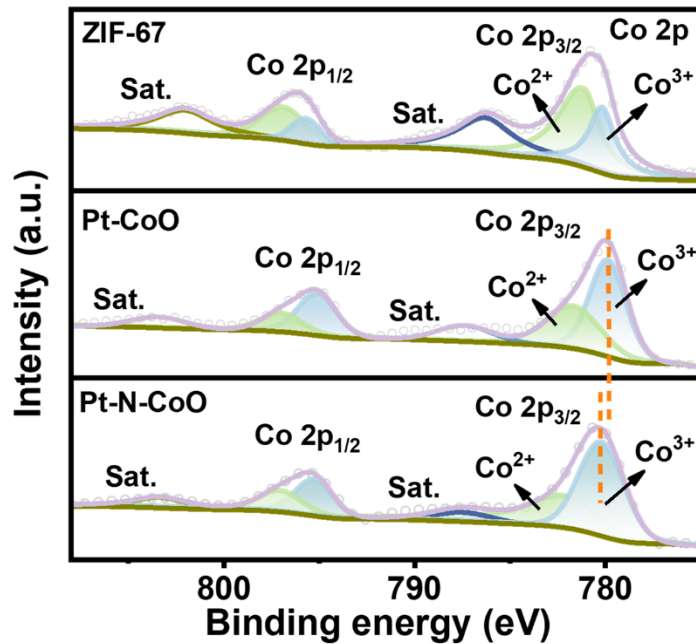
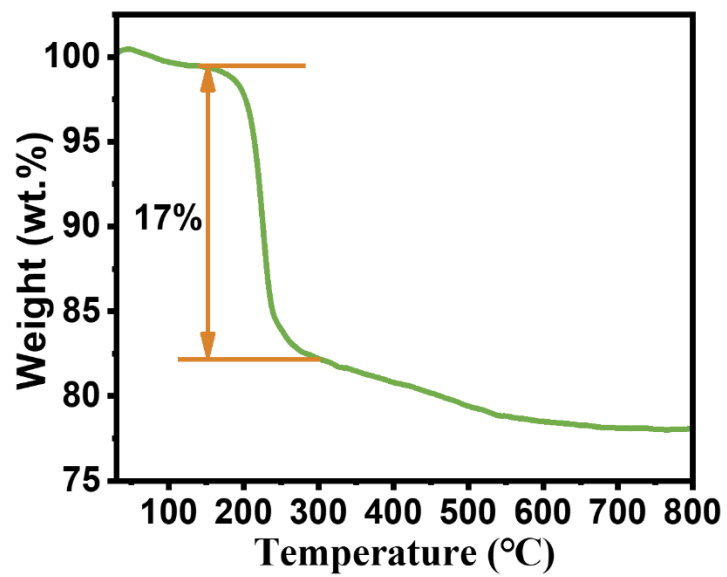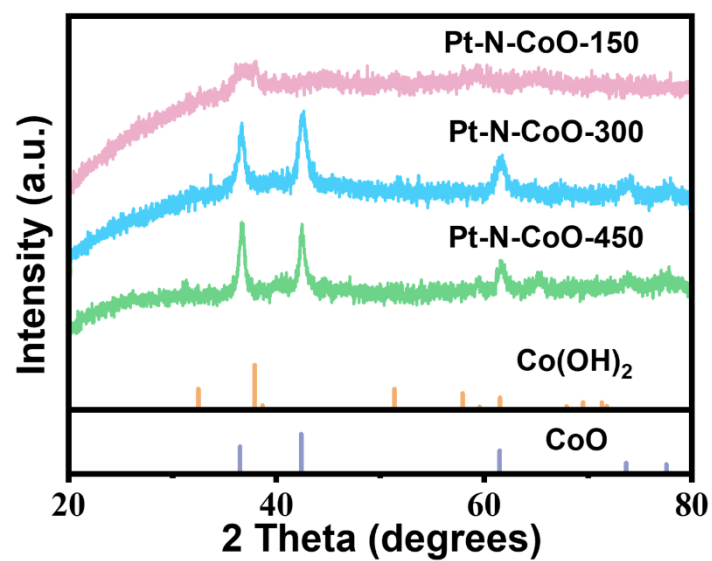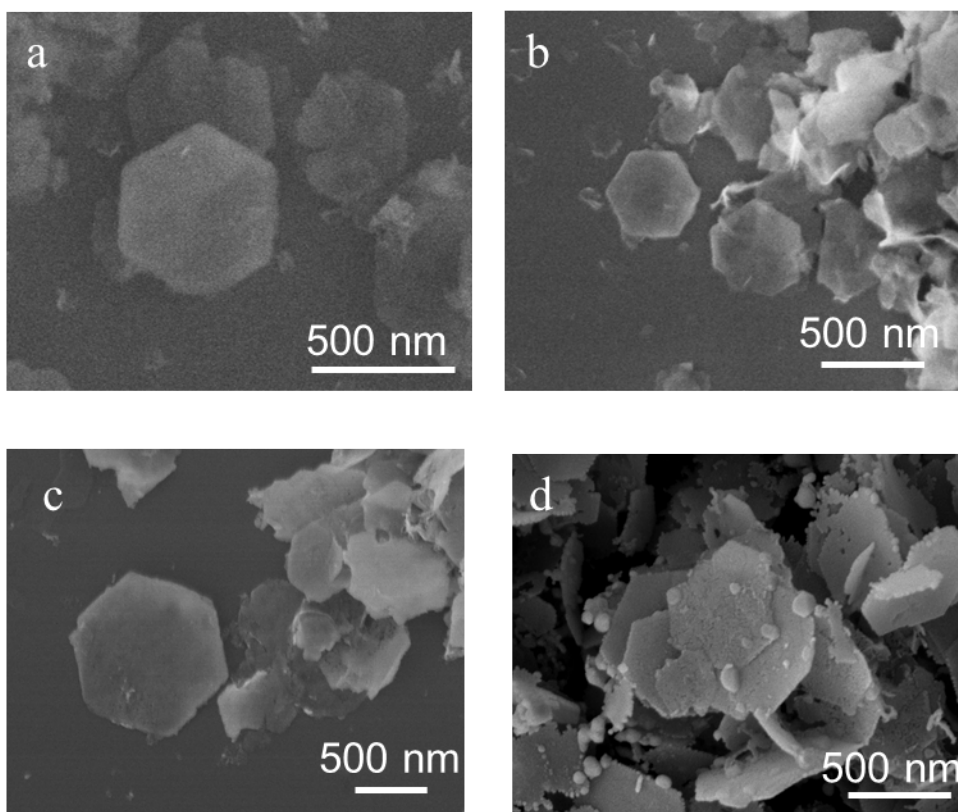**Fig.S1.** XPS spectra of Co 2*p* spectrum for ZIF-67, Pt-CoO and Pt-N-CoO.

Fig.S2. The thermogravimetry of Pt-N-Co(OH)$_2$

Fig.S3. XRD of Pt-N-Co(OH)$_2$, Pt-N-Co(OH)$_2$-150, Pt-N-Co(OH)$_2$-300, Pt-N-Co(OH)$_2$-450

Fig.S4. SEM of Pt-N-Co(OH)$_2$ (a), Pt-N-Co(OH)$_2$-150 (b), Pt-N-Co(OH)$_2$-300 (c), Pt-N-Co(OH)$_2$-450 (d)
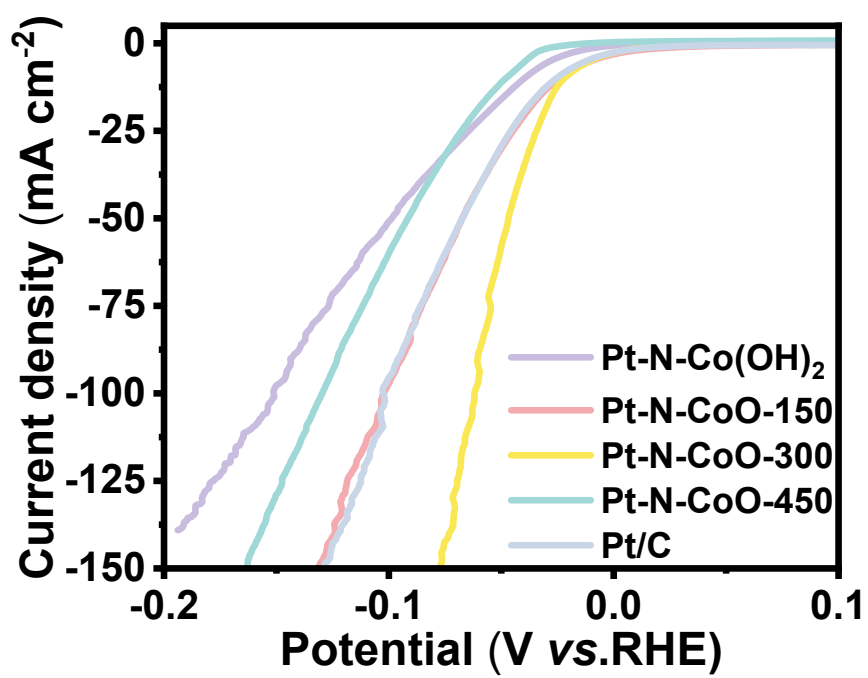
Fig.S5. LSV curves of Pt-N-Co(OH)$_2$,Pt-N-CoO-150,Pt-N-CoO-300,Pt-N-CoO-450 and Pt/C
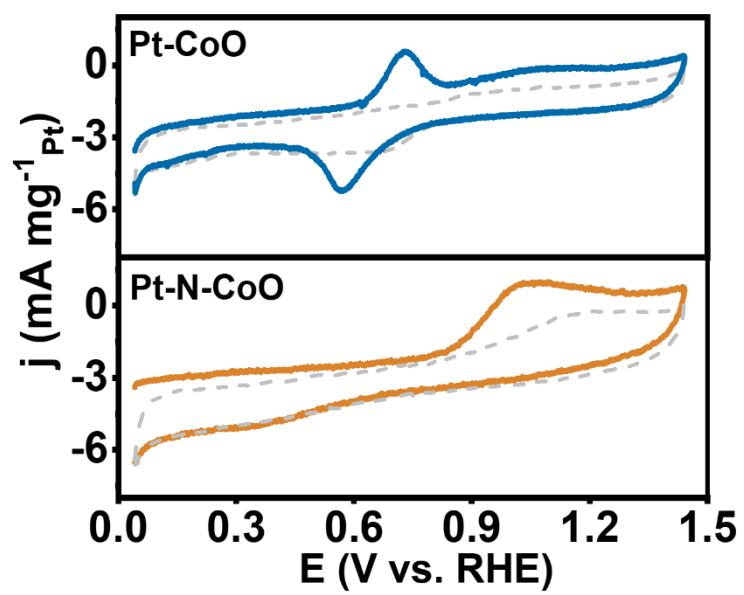
Fig.S6. CO stripping voltammetry of Pt-CoO and Pt-N-CoO
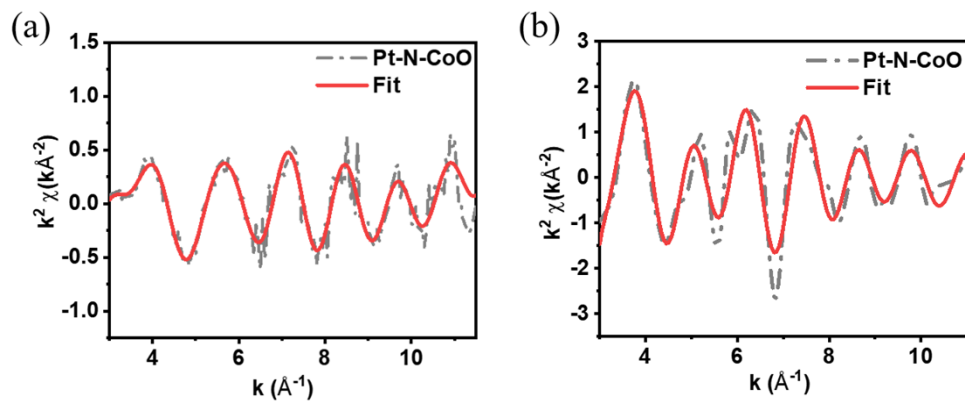
Fig. S7. The Pt L_3-edge(a) and Co K-edge (b) $k^2\chi(k)$ oscillations.
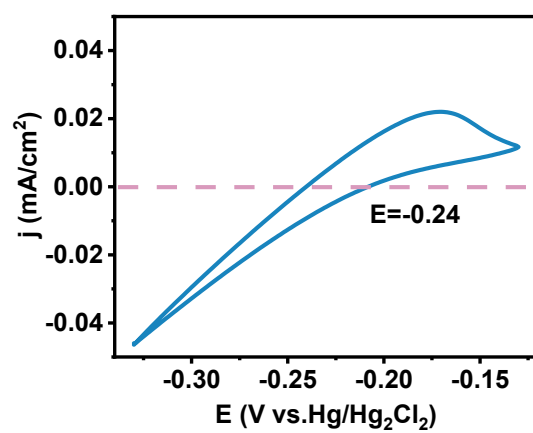
Fig.S8 Current-potential curve for the calibration of the Hg/Hg_2Cl_2 with respect to the RHE in high-purity, hydrogen saturated: 0.05 M H_2SO_4 solution using Pt foil as the working electrode and counter electrode.

Table S1. The weight percent of Pt and Co by ICP-MS measurement

	Pt (w%)	Co (w%)
Pt-CoO	6.2	62.7
Pt-N-CoO	6.0	73.6

Table S2. The comparison of HER performances of Pt-N-CoO and other HER catalysts.

| Catalysts	Potential at 10 mA cm^{-2}(V)	Tafel slope (mV dec^{-1})	Ref.
La$_2$Sr$_2$PtO$_{7+\delta}$	13	22	1
PtRu@RFCS	20	27.2	2
MoS$_x$/CNTs/Pt	25	27	3
Pt@Co SAs-ZIF-NC	27	21	4
Mo$_2$TiC$_2$Tx-Pt SA	30	30	5
Pt@C$_2$N	40	31	6
Pt-WO$_3$	31	32	7
Pt-CoO/p-CNF	26	31.5	8
Er-WS$_2$-Pt	27	40	9
PtCoNi FNs	41	37	10
Pt/RuCeOx	45	31	11
Pt-MoS$_2$	53	40	12
Pt SA/m-WO$_{3-x}$	47	45	13
Pt/C	24	32	
This work	22	33	

Table S3. EXAFS fitting parameters at the Co K and Pt $L3$ edge (S_0^2=1.262, 0.826)

	Path	C.N.	R (Å)	$\sigma^2 \times 10^3$(Å^2)	ΔE (eV)	R factor
Co foil	Co-Co	12*	2.49	6.3	7.321	0.0015
CoO	Co-O	3.7	2.13	6.2	1.7	0.010
	Co-Co	11.1	3.00	8.6	-3.5	
Pt-CoO	Co-O	5.6	2.13	23.21	9.188	0.019
	Co-Co	5.6	2.64	27.43		
	Co-Pt	11.4	2.79	11.43		
Pt-N-CoO	Co-O	7.1	2.18	9.62	9.384	0.0054
	Co-Co	7.1	2.74	8.26		
	Co-Pt	14.3	2.68	40.0		
	Co-N	7.1	2.48	7.03		

	Path	C.N.	R (Å)	$\sigma^2 \times 10^3$(Å^2)	ΔE (eV)	R factor
Pt foil	Pt-Pt	12*	2.76	4.27	7.565	0.0035
Pt-CoO	Pt-O	4.4	2.04	36.93	3.750	0.00013
	Pt-Pt	4.4	2.68	4.47		
	Pt-Co	8.7	2.56	28.82		
Pt-N-CoO	Pt-O	4.2	2.12	18.20	2.046	0.0010
	Pt-Pt	4.2	2.65	7.18		
	Pt-Co	8.3	2.58	38.85		
	Pt-N	4.2	1.91	21.92		

C.N.: coordination numbers; R: bond distance; σ^2: Debye-Waller factors; ΔE: the inner potential correction. R factor: goodness of fit. * fitting with fixed parameter.

1.   J. Dai, Y. Zhu, Y. Chen, X. Wen, M. Long, X. Wu, Z. Hu, D. Guan, X. Wang, C. Zhou, Q. Lin, Y. Sun, S.-C. Weng, H. Wang, W. Zhou and Z. Shao, *Nat. Commun.*, 2022, **13**, 1189.
2.   K. Li, Y. Li, Y. Wang, J. Ge, C. Liu and W. Xing, *Energy Environ. Sci.*, 2018, **11**, 1232-1239.
3.   Y. Zhan, Y. Li, Z. Yang, X. Wu, M. Ge, X. Zhou, J. Hou, X. Zheng, Y. Lai, R. Pang, H. Duan, X. a. Chen, H. Nie and S. Huang, *Adv. Sci.，* 2019, **6**, 1801663.
4.   L. Liang, H. Jin, H. Zhou, B. Liu, C. Hu, D. Chen, Z. Wang, Z. Hu, Y. Zhao, H.-W. Li, D. He and S. Mu, *Nano Energy*, 2021, **88**, 106221.
5.   J. Zhang, Y. Zhao, X. Guo, C. Chen, C.-L. Dong, R.-S. Liu, C.-P. Han, Y. Li, Y. Gogotsi and G. Wang, *Nat. Catal.*, 2018, **1**, 985-992.
6.   D. Li, M. Chen, Z. Sun, P. Yu, Z. Liu, P. M. Ajayan and Z. Zhang, *Nat. Nanotechnol.*, 2017, **12**, 901-906.
7.   C. Xie, W. Chen, S. Du, D. Yan, Y. Zhang, J. Chen, B. Liu and S. Wang, *Nano Energy*, 2020, **71**, 104653.
8.   Y. Li, R. Cao, L. Li, X. Tang, T. Chu, B. Huang, K. Yuan and Y. Chen, Small, 2020, 16, 1906735.
9.   C. X. Zhao, J.-N. Liu, B.-Q. Li, D. Ren, X. Chen, J. Yu and Q. Zhang, Adv. *Funct. Mater.*, 2020, **30**, 2003619.
10.   M. T. Liu, L.-X. Chen, A.-J. Wang, K.-M. Fang and J.-J. Feng, *Int. J. Hydrogen Energy*, 2017, **42**, 25277-25284.
11.   T. Liu, W. Gao, Q. Wang, M. Dou, Z. Zhang and F. Wang, *Angew. Chem. Int. Ed. Engl.*, 2020, **59**, 20423-20427.
12.   X. Y. Xu, X. F. Dong, Z. J. Bao, R. Wang, J. G. Hu and H. B. Zeng, J. *Mater. Chem. A.*, 2017, **5**, 22654-22661.
13.   J. Park, S. Lee, H. E. Kim, A. Cho, S. Kim, Y. Ye, J. W. Han, H. Lee, J. H. Jang and J. Lee, *Angew. Chem. Int. Ed. Engl.*, 2019, **58**, 16038-16042.